Hindawi
Mathematical Problems in Engineering
Volume 2021, Article ID 6645128, 10 pages
https://doi.org/10.1155/2021/6645128

Research Article

Computational Fluid Dynamics Analysis of Flow Patterns, Pressure Drop, and Heat Transfer Coefficient in Staggered and Inline Shell-Tube Heat Exchangers

Shubham Sharma,[1] **Shalab Sharma**,[2] **Mandeep Singh**,[3] **Parampreet Singh**,[4] **Rasmeet Singh**,[5] **Sthitapragyan Maharana**,[6] **Nima Khalilpoor**,[7] **and Alibek Issakhov**[8]

[1]*Department of Mechanical Engineering, IKG Punjab Technical University, Jalandhar-Kapurthala Road, Kapurthala 144603, Punjab, India*
[2]*Department of Mechanical Engineering, DAV University, Jalandhar, Punjab, India*
[3]*School of Mechanical and Mechatronic Engineering, University of Technology Sydney, Sydney, NSW, Australia*
[4]*Department of Mechanical Engineering, Guru Nanak Dev University, Amritsar, India*
[5]*Dr. S.S. Bhatnagar University Institute of Chemical Engineering & Technology, Panjab University, Chandigarh 160 014, India*
[6]*University of Technology Sydney, Sydney, NSW, Australia*
[7]*Department of Energy Engineering, Graduate School of the Environment and Energy, Science and Research Branch, Islamic Azad University, Tehran, Iran*
[8]*Faculty of Mechanics and Mathematics, Department of Mathematical and Computer Modelling, Al-Farabi Kazakh National University, Almaty, Kazakhstan*

Correspondence should be addressed to Shubham Sharma; shubham543sharma@gmail.com and Nima Khalilpoor; nimakhalilpoor@gmail.com

Received 16 November 2020; Revised 28 April 2021; Accepted 18 May 2021; Published 1 June 2021

Academic Editor: Younes Menni

In this numerical study, the heat transfer performance of shell-and-tube heat exchangers (STHXs) has been compared for two different tube arrangements. STHX having 21 and 24 tubes arranged in the inline and staggered grid has been considered for heat transfer analysis. Shell-and-tube heat exchanger with staggered grid arrangement has been observed to provide lesser thermal stratification as compared to the inline arrangement. Further, the study of variation in the mass flow rate of shell-side fluid having constant tube-side flow rate has been conducted for staggered grid structure STHX. The mass flow rate for the shell side has been varied from 0.1 kg/s to 0.5 kg/s, respectively, keeping the tube-side mass flow rate as constant at 0.25 kg/s. The influence of bulk mass-influx transfer rate on heat transfer efficiency, effectiveness, and pressure drop of shell-tube heat exchangers has been analyzed. CFD results were compared with analytical solutions, and it shows a good agreement between them. It has been observed that pressure drop is minimum for the flow rate of 0.1 kg/s, and outlet temperatures at the shell side and tube side have been predicted to be 40.94°C and 63.63°C, respectively.

1. Introduction

Heat transfer analysis of shell-tube heat exchangers is critical owing to their applications in many of the engineering domains like energy production, industrial chemistry, bionics, nanotechnology applications, air conditioning, refrigeration, and food industries [1–3]. It has been reported that around 35% of the total heat exchangers are STHXs [4]. STHX of various sizes is used widely in many industrial applications [3, 5, 6]. The layout model of draft-structure configurations of the shell-and-tube heat exchanger may vary according to the need. Tubular Exchanger Manufacturers Association (TEMA) publishes the standardizing norms or regulations and design configurations regularly.

The Bureau of Indian Standards also suggested a design configuration and standards for shell-and-tube heat exchangers [7]. The shell-side flow inside the STHX is very complicated due to bypass between different flow zones and leakages. The effect of leakages and bypass on the performance of STHX may vary for different shell designs and sizes [8, 9]. Several studies put shell-and-tube heat exchangers in the area of focus due to their vast utilization in the industry, especially in the oil and gas industry [10–12]. Bhuyian et al. [13] reviewed the performance of plate-fin and tubular heat exchangers. Costa and Queiroz [14] investigated the design optimization procedure of the STHX to minimize the thermal surface area. Jozaie et al. [15] investigated the effect of baffle spacing on the heat transfer rate, pressure drop, and cost of the STHX and concluded that the optimal baffle spacing to achieve a higher heat transfer rate, lower pressure drops, and cost would be around 8–12 inches. Li and Kottke [16] studied the variation of baffle spacing on pressure drop and heat transfer coefficient of STHX with staggered tube layout. Rai et al. [17] performed a parametric study on the STHX and monitored that the tube pitch ratio is the main factor for the thermal performance of STHXs. Patel et al. [18] reviewed all the CFD-based studies investigating the heat transfer in the STHXs. Lebele-Alawa and Egwanwo [19] numerically investigated the heat transfer in the heat exchangers and reported high efficiency and accuracy for the presented numerical model. Chalwa and Kadli [20] investigated the effect of vertical baffles on the heat transfer performance and pressure drop of the STHXs. Anand et al. [21] used the Bell-Delaware method to perform an experimental investigation on the performance of STHXs. Yang et al. [22] compared four modeling methods and validated the compared models with experimental results for the rod baffle heat exchangers. Wang et al. [23] studied the effect of installing sealers on the shell side of the STHX. They reported a considerable enhancement in the heat transfer coefficient and energy efficiency of the STHX. Ramezanpour et al. [24] investigated the effect of the staggered tube bundle in a turbulent cross-flow regime to find the optimal layout. Kwak et al. [25] varied the number of tube rows of staggered finned tube bundles and studied their effect on the heat transfer rate and pressure drop. It has been inferred that three rows of tube bundles obtained the least pressure drop among other tested schemes. Beale and Spalding [26] compared the performance of STHX for inline and staggered tube banks under transient flow conditions. Jayawel and Tiwari [27] performed a similar study and compared the performance of inline and staggered tube banks in a 3D model and validated the obtained results with the data available in the literature and reported high accuracy for the presented code.

In the present study, two different types of shell-and-tube heat exchangers, one with an inline tube structure and the other with staggered tube structure, have been studied numerically for heat transfer performance. CFD simulations were performed to analyze the heat transfer efficacy of both heat exchangers. A shell-tube heat exchanger with a staggered grid structure resulted in improvements in heat transfer performance, so it has been considered for further analysis. In the second phase of the study, variation in the bulk mass-transfer flow rate of lateral shell-face fluid has been analyzed, keeping the tube-side flow rate as fixed at 0.25 kg/s. The results and conclusions have been drawn based on the observed outcomes of heat transfer under different bulk mass flow rates varying from 0.1 kg/s to 0.5 kg/s. With the advancement of computer programming and technology, numerical simulation has replaced prototype testing. Nowadays, numerical simulations are being conducted to optimize the efficiency of various devices, tools, and equipment [28–33]. To perform the study, numerical simulation has been done on 3D geometry of STHX using ANSYS FLUENT 15 to know the effect of variation in mass flow rate of shell-tube sided and arrangements of conduit-tube wads or bales in the heat exchangers. CFD results have also been compared with the analytical solutions, and the differences observed have been examined.

2. Modeling Details

In this study, the tubes of shell-tube heat exchangers have been arranged in two different configurations, inline structure and staggered structure having 21 and 24 numbers of tubes, respectively. The shell has dimensions of 94.7 mm in diameter and 810.1 mm in length. Likewise, the outer and inner diameters of the tubes are 12.5 mm and 11 mm, respectively. Water has been considered as drive operating medium fluid for both shell and tube sides. The physical properties of water have been considered as those given in the Fluent database.

2.1. Governing Equations. Steady and incompressible flow conditions have been assumed for the sake of simplifying the numerical analysis. The mass flow rates used in the present study correspond to turbulent flow conditions, and thus turbulence modeling has been done using the two-equation "k-ε" turbulence model. The "k-ε" turbulence model has been used due to its versatility and robustness in handling a wide range of turbulent flows. At the same time, the model is stable and poses lesser convergence difficulties. The governing equations for the flow are given as follows [23–28, 34].

$$\text{Conservation of mass}: \ \nabla.(\rho\vec{V}) = 0. \tag{1}$$

Momentum equation:

X-momentum:

$$\nabla.(\rho u\vec{V}) = -\frac{\partial p}{\partial x} + \frac{\partial \tau_{xx}}{\partial x} + \frac{\partial \tau_{xy}}{\partial y} + \frac{\partial \tau_{xz}}{\partial z}. \tag{2}$$

Y-momentum:

$$\nabla.(\rho v\vec{V}) = -\frac{\partial p}{\partial y} + \frac{\partial \tau_{xy}}{\partial x} + \frac{\partial \tau_{yy}}{\partial y} + \frac{\partial \tau_{zy}}{\partial z} + \rho g. \tag{3}$$

Z-momentum:

$$\nabla.(\rho w\vec{V}) = -\frac{\partial p}{\partial z} + \frac{\partial \tau_{xz}}{\partial x} + \frac{\partial \tau_{yz}}{\partial y} + \frac{\partial \tau_{zz}}{\partial z} \quad (4)$$

Energy equation:

$$\nabla.(\rho e\vec{V}) = -p\nabla.\vec{V} + \nabla.(k\nabla T) + q + \varnothing, \quad (5)$$

where "Ø" is the dissipation function and can be calculated from [23–28, 34]

$$\varnothing = \mu\left[2\left\{\left(\frac{\partial u}{\partial x}\right)^2 + \left(\frac{\partial v}{\partial y}\right)^2 + \left(\frac{\partial w}{\partial z}\right)^2\right\} + \left(\frac{\partial u}{\partial y} + \frac{\partial v}{\partial x}\right)^2 + \left(\frac{\partial u}{\partial z} + \frac{\partial w}{\partial x}\right)^2 + \left(\frac{\partial v}{\partial z} + \frac{\partial w}{\partial y}\right)^2\right] + \lambda(\nabla.\vec{V})^2. \quad (6)$$

2.2. Geometry. The geometry of STHX has been modeled in SolidWorks, and Table 1 describes the dimensions of the heat exchanger. The schematic of STHX with a staggered grid structure and inline grid structure is presented in Figures 1(a) and 1(b). In the present work, the cold fluid has been made to flow in the tubes and hot fluid through the shell. It can also be seen that there are two baffles provided in the shell of the STHX heat exchanger.

2.3. Mesh Generation. The tetrahedral mesh has been generated using Fluent Meshing. The grid generated has been analyzed for aspect ratio and orthogonal quality. The computational grid for STHX has approximately 17,622,730 and 18,233,589 grid elements for the inline and staggered grid. The aforementioned grid density has been obtained after carrying out the necessary grid convergence test.

2.4. Boundary Conditions. The inlet mass flow rate and inlet temperature values have been assigned to the STHX. The shell fluid inlet temperature has been considered as 20°C, and the tube-side fluid inlet temperature is 80°C.

Gauge pressure has been considered to be zero at the outlet. The velocity profile has been assumed to be uniform for simplifying the calculations. The no-slip condition has been considered for all the wall surfaces, and the heat flux value has been assigned as zero for the outer surface of the shell, i.e., the shell-side outer surface has been considered as adiabatic (Table 2).

2.5. Turbulence Model. The mass flow rate used for the flowing stream corresponds to turbulent flow conditions, and hence turbulent effects cannot be ignored. The standard "k-ε" model has been employed for the turbulent transport analysis. The two-equation "k-ε" turbulence model has been used due to its simplicity and faster convergence as compared to other models. In the past literature available on In previous research on CFD studies, the "k-ε" model has been used for almost every flow situation. Thus, the same model has been considered as well. For steady-state conditions, the model equations are [23–29, 34]

Table 1: Design parameters for shell-tube heat exchangers.

Parameters	Design values
Shell diameter, D_s	94.7 mm
Outer-tube diameter, d_o	12.5 mm
Bunch-tube bale structure	Inline and staggered
Pitch	1.5625 cm
Number of tubes, N_t	21 and 24
Heat exchanger length, L	810 mm
Number of baffles, N_b	2
Shell fluid inlet temp., T_{cin}	20°C
Tube fluid inlet temp., T_{hin}	85°C

$$\frac{\partial}{dx_i}(\rho k u_i) = \frac{\partial}{dx_j}\left[\left(\mu + \frac{\mu_t}{\sigma_k}\right)\frac{\partial k}{\partial x_j}\right] + G_k + G_b - \rho\varepsilon + S_k, \quad (7)$$

$$\frac{\partial}{dx_i}(\rho\varepsilon u_i) = \frac{\partial}{dx_j}\left[\left(\mu + \frac{\mu_t}{\sigma_\varepsilon}\right)\frac{\partial \varepsilon}{\partial x_j}\right] + C_{1\varepsilon}\frac{\varepsilon}{k}(G_k - C_{3\varepsilon}G_b) - C_{2\varepsilon}\rho\frac{\varepsilon^2}{k} + S_\varepsilon, \quad (8)$$

$$\mu_t = \rho C_\mu \frac{k^2}{\varepsilon}. \quad (9)$$

Equations (7) and (8) are the transport equations for k and ε, and equation (9) is the equation for turbulent eddy viscosity. In equation (7), $i = 1$, $j = 1$, 2, and 3 represents the space variables in "x," "y," and "z" directions, and the model constants values used in the turbulence model are $C_{1\&\varepsilon} = 1.44$, $C_{2\&\varepsilon} = 1.92$, $C_\mu = 0.09$, $\sigma_k = 1.0$, and $\sigma_{\&\varepsilon} = 1.3$.

3. Results and Discussion

The numerical analysis has been carried out on STHX with inline and staggered tube structure, and a comparison of results shows that the performance of STHX is better with staggered tube structure than that with the inline tube structure. Outlet temperature for shell and tube side is given in Table 3. The effectiveness for the staggered and inline tube heat exchangers is 64.10% and 53.15%, respectively. Based on effectiveness, it is evident that staggered tube heat exchanger is more efficient as compared with aligned tube-conduit heat exchanger, so further calculations have been performed on staggered grid shell-tube type heat exchanger only.

From the results, it can be clearly identified that the heat transfer performance of shell-tube type heat exchanger with staggered grid structure is better than the heat exchanger with inline grid structure (Figures 2(a)–2(c) and Figures 2(d)–2(f)). So, for further analysis of variation in bulk mass-influx flow rate for shell fluid, shell-and-tube heat exchanger with staggered grid structure has been considered. Mass flow rate of shell-side fluid has been varied from

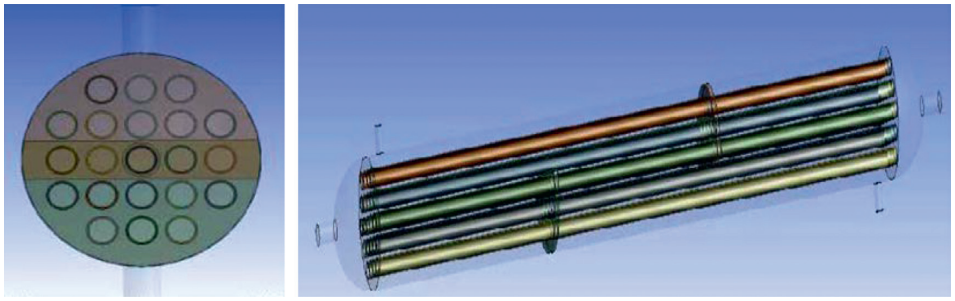

(a)

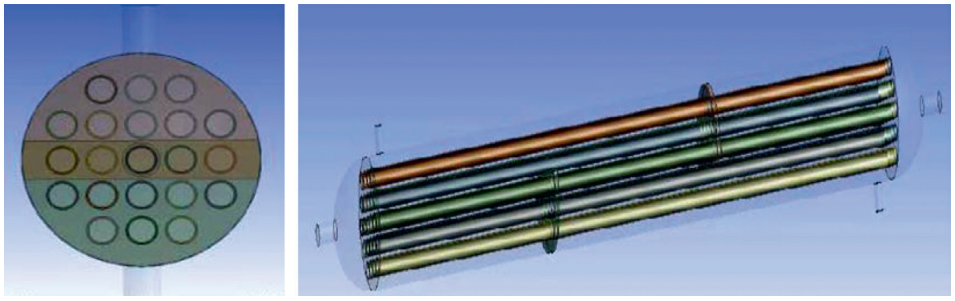

(b)

Figure 1: (a) STHX with staggered grid structure. (b) STHX with inline grid structure.

Table 2: Boundary conditions applied at various faces.

Sr. No.	Physical location	Boundary condition
1	Shell wall	Adiabatic wall boundary condition (no slip) ($\dot{q}'' = 0$; $u = v = w = 0$)
2	Baffle walls	Wall boundary condition (no slip) ($T_b = T_{atm} = 27^{\circ}\text{C}$; $u = v = w = 0$)
3	Shell outlet	Pressure outlet ($P = P_{atm}$; $T = T_{atm}$)
4	Tube outlet	Pressure outlet ($P = P_{atm}$; $T = T_{atm}$)
5	Pipe walls	Conjugate heat transfer
6	Inlets	Mass flow inlets (corresponding to 0.1 kg/s–0.5 kg/s for shell side having fixed inlet temperature $T_{cin} = 20^{\circ}\text{C}$ and 0.25 kg/s for tube side with fixed $T_{hin} = 85^{\circ}\text{C}$)

Table 3: Outlet temperatures of shell-tube heat exchanger.

Zone	STHX with inline tube structure (°C)	STHX with staggered tube structure (°C)
Shell inlet	20.00	20.00
Shell outlet	35.33	42.93
Tube inlet	85.00	85.00
Tube outlet	50.45	43.33

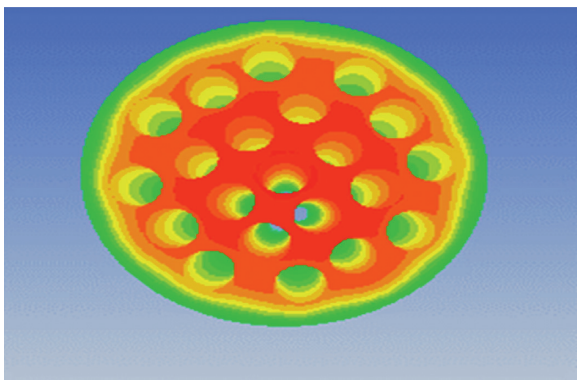

(a)

Figure 2: Continued.

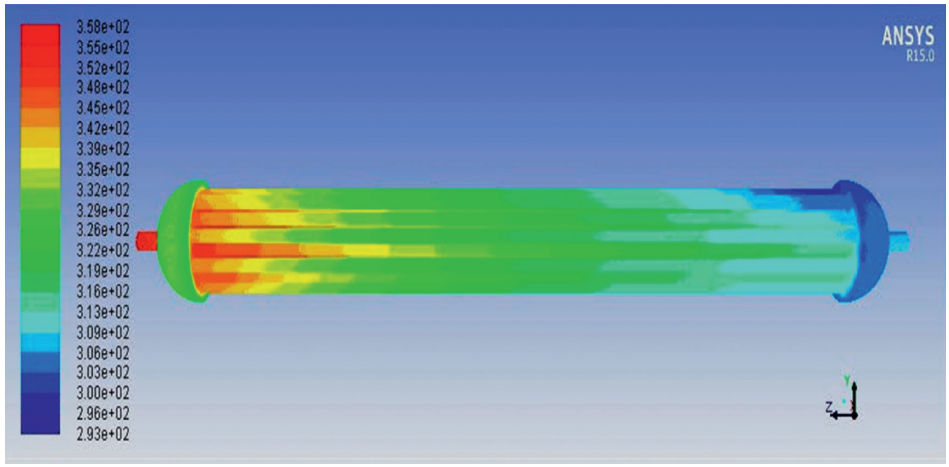

(b)

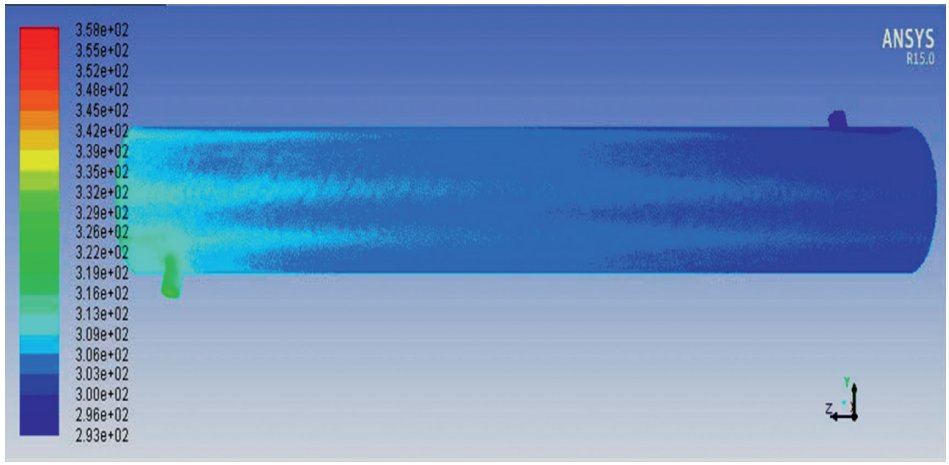

(c)

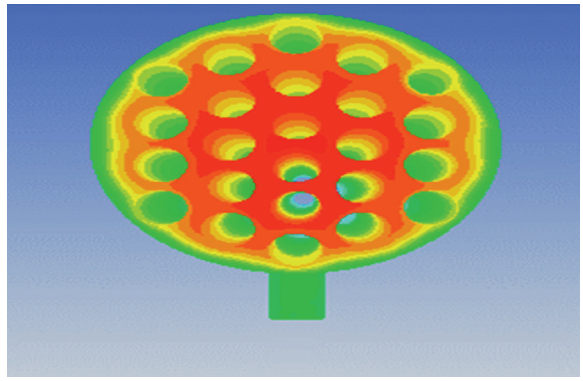

(d)

Figure 2: Continued.

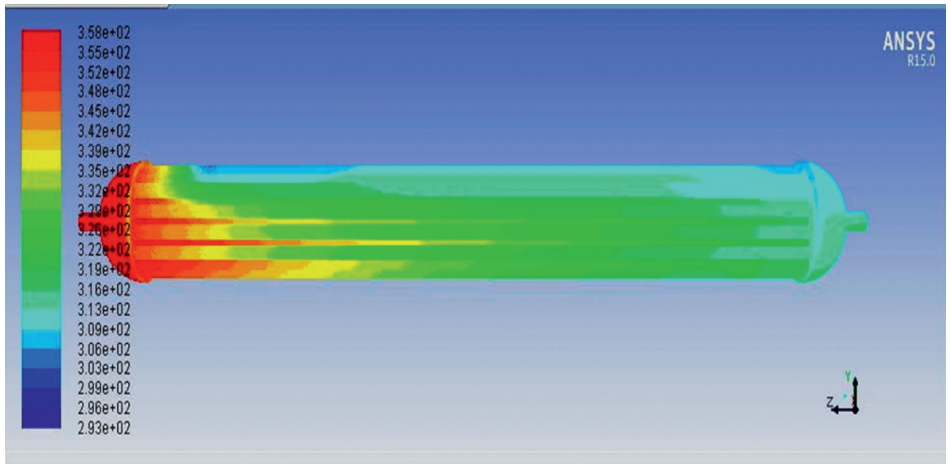

(e)

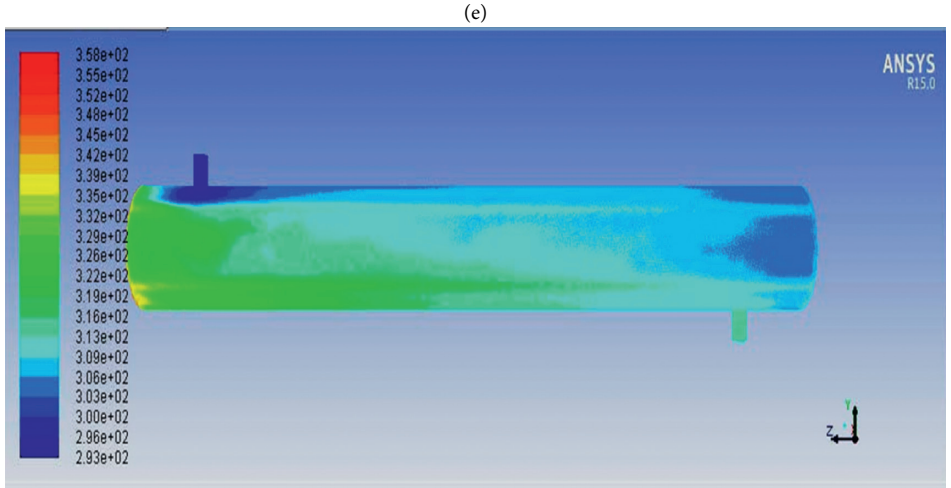

(f)

Figure 2: Static temperature variation in STHX with (a–c) inline grid and (d–f) staggered grid.

Table 4: CFD results for variation in mass flow rate.

Mass flow rate (kg/s)	Outlet temperatures (°C)		Heat transfer coefficient (W/m^{2}K)	Shell-side pressure drop (Pa)	Rate of heat transfer (W)
	T_c	T_h			
0.1	40.94	63.63	714.33	450.9	8750
0.2	32.63	70.90	1045.84	530.4	10557
0.3	29.12	74.05	1307.12	648.6	11443
0.4	27.17	75.53	1531.20	710.1	11989
0.5	25.92	77.17	1731.15	862.2	12365

0.1 kg/s to 0.5 kg/s, and tube-side flow has been taken as constant at 0.25 kg/s.

Table 4 describes the outlet temperatures of the shell-tube heat exchanger for changing mass flow rates. Shell fluid inlet and tube fluid inlet temperatures are kept identical for all cases, which correspond to 20°C and 85°C, respectively. Table 5 describes the effect of variation in mass flow rate on flow parameters such as pressure drop and heat transfer characteristics using respective analytical formulas.

Table 6 presents the percentage discrepancy among the CFD predictions and analytical outcomes by taking the

Table 5: Analytical calculations for variation in mass flow rate on flow and heat transfer.

Mass flow rate (kg/s)	Heat transfer coefficient (W/m^{2}K)	Shell-side pressure drop (Pa)	Rate of heat transfer (W)
0.1	607.11	414.83	7262.5
0.2	941.04	498.57	9739.6
0.3	1202.55	616.17	10921.8
0.4	1453.11	674.95	11624.4
0.5	1678.69	810.46	11991.6

Table 6: Percent difference between CFD analysis and analytical calculations.

Mass flow rate (kg/s)	Heat transfer coefficient (W/m^{2}K)	Shell-side pressure drop (Pa)	Rate of heat transfer (W)
0.1	15.01	8.01	4.88
0.2	10.02	6.20	8.39
0.3	8.00	5.00	4.77
0.4	5.10	4.95	3.13
0.5	3.03	6.00	3.11

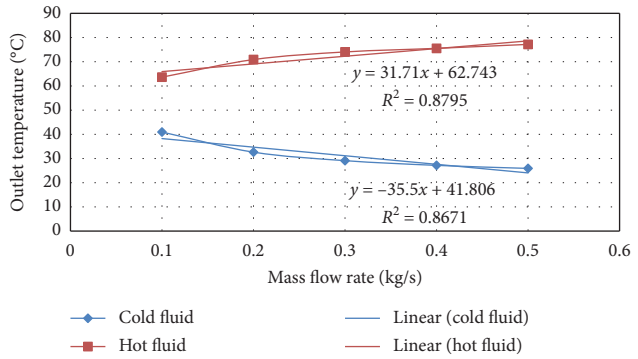

Figure 3: Effect of outlet temperature (°C) against the mass flow rate (Kg/s).

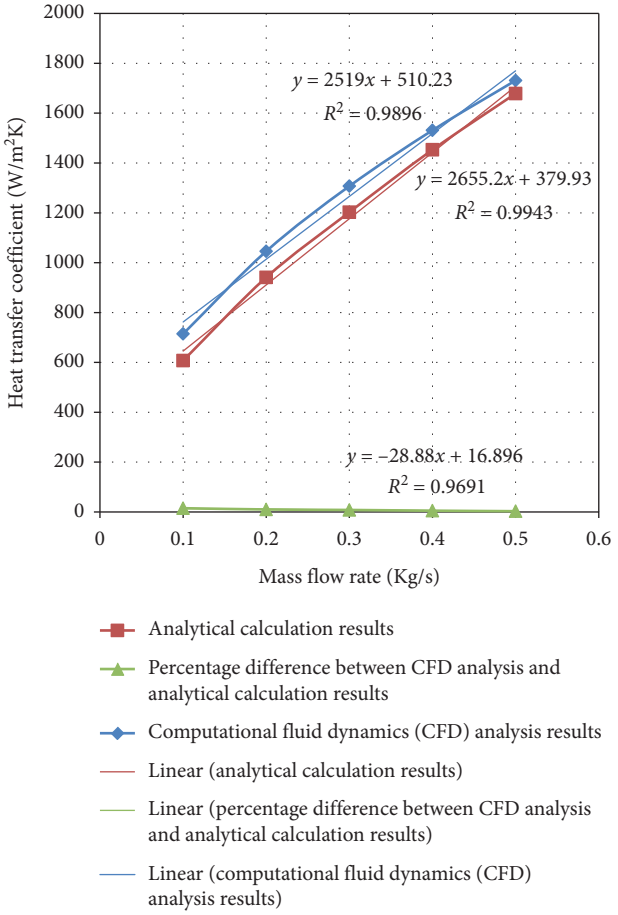

Figure 4: Effect of heat transfer coefficient (W/m^{2}K) against the mass flow rate (Kg/s).

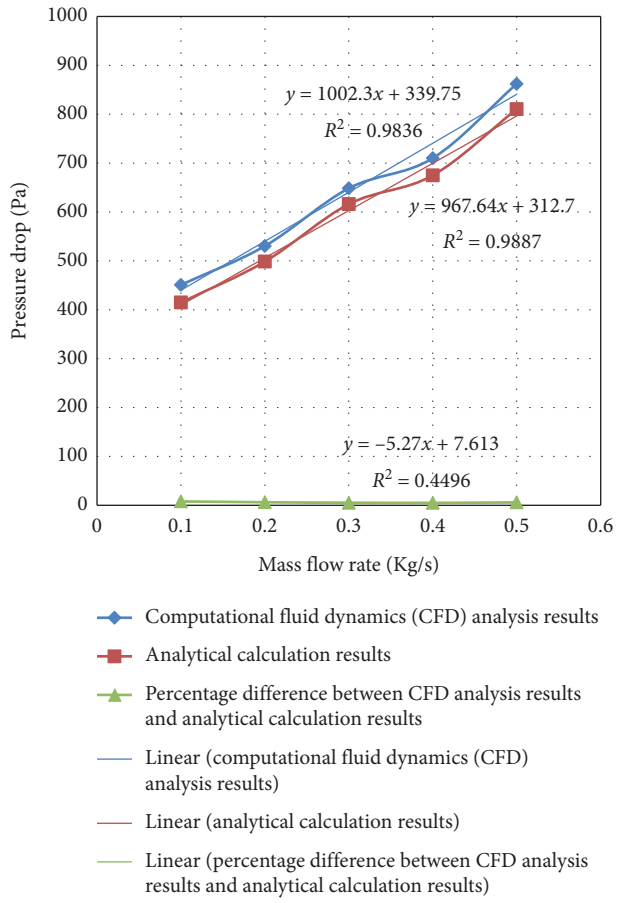

Figure 5: Effect of pressure drop (Pa) against the mass flow rate (Kg/s).

standard analytical results for pressure drop and heat transfer coefficient occurring in internal flows as reference. With the increase in the mass flow rate of shell fluid, both the heat transfer coefficient and pressure drop increase, but the outlet temperature of hot and cold fluid decreases, which ultimately reduces the potential efficiency of a shell-tube heat exchanger. The above results show good agreement between CFD and analytical solutions, and a maximum difference of 15.01% has been noticed in the heat transfer coefficient at the lowest flow rate.

The graphical representation, as illustrated in Figures 3–6, exhibits the influence of mass flow rate variations on outlet temperatures of STHX, pressure drop, heat transfer coefficient, and rate of heat transfer. It has been observed that an increase in mass flow rate of shell fluid leads to a decrease in outlet temperatures of a shell-tube heat exchanger and enhancement of both pressure drop as well as

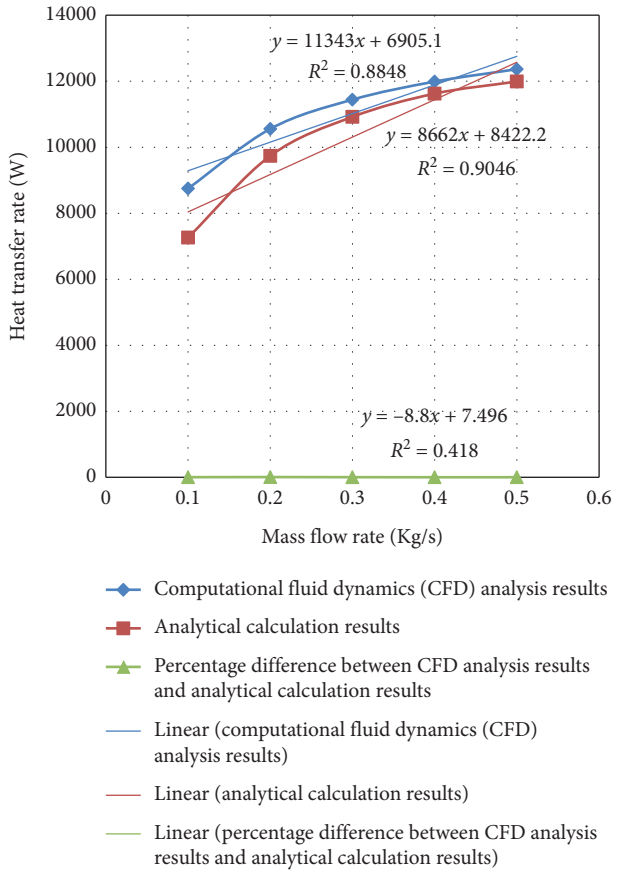

Figure 6: Effect of rate of heat transfer (W) against the mass flow rate (Kg/s).

heat transfer coefficient. The enhancement of pressure drop is expected because of the turbulence in a flow field. The related investigation was reported by Singh et al., which analyzed that the Reynolds averaged N-S eqns.-predicated turbulent simulation in commercial C. F. D. Fluent was being employed for numerical analysis. The three-distinct "k-ε," as well as the shearing-stress-transport (S.S.T.) "k-ω" models, are being used in the analysis. In order to determine the best-efficient and reliable turbulence model, the numerical simulation efficiency analysis was compared with empirical outcomes. For the design topography and configuration in consideration, the influence of alteration of Reynolds number ($\mathrm{Re_p}$), interjet, and separation distance was being contemplated. Such factors influenced the heat transfer coefficient, temp., and turbulence intensity in a stream. Results revealed that the localized "h" levels were being considerably decreased as the separation distance "non-dimensional-impingement separation H/D " escalates. The S.S.T. "k-ω" design model had been reported to be the least important determinant and reliable assessment of empirical outcomes. With an improvement in "H/D" from six-to-ten at "$\mathrm{Re_p}$" $= 9 \times 10^3$ and "interjet-spacing, S/D " of three, the mean of heat transfer performance "h" significantly decreases from 0.021 to 0.0193 W/cm^{2}K. The interjet spacing "S/D " of three was being computed to be the more optimal value predicated upon analytical findings as unveiled by the Singh et al. [34].

4. Conclusions

The STHX has been modeled with staggered and inline tube structures to analyze the heat transfer performance. From the CFD simulations for the shell-tube heat exchanger, outlet temperatures of shell-tube fluids and their effectiveness have been obtained. From the obtained results, the following conclusions can be drawn:

(a) STHX with staggered tube structure is better than the STHX with inline tube structure.

(b) Effect of variation in shell fluid mass flow rate has been analyzed on heat transfer rate, pressure drop, heat transfer coefficient, and outlet temperatures of shell-tube heat structure by varying the shell-side mass flow rate from 0.1 kg/s to 0.5 kg/s and keeping tube-side flow rate as constant at 0.25 kg/s. The results show that with the rise in shell-side mass flow rate, both the pressure drop and heat transfer coefficient enhance and decrease the outlet temperatures.

(c) It has been observed that pressure drop is minimum for a mass flow rate of 0.1 kg/s, and outlet temperatures at the shell side and tube side are 40.94°C and 63.63°C, respectively. The increase in pressure drop for increasing mass flow rate has been attributed to the turbulence, and thus higher shear stresses exist at the surfaces.

(d) It has been observed that there is an excellent accord among CFD and analytical findings. The percentage difference between analytical solution and CFD simulation results shows the highest difference of 15.01% for heat transfer coefficient, 8.01% for shell-side pressure drop, and 8.39% for heat transfer rate.

Abbreviations

x, y, z: Coordinate axis
D_s: Shell diameter (mm)
d_i: Inner diameter of tube (mm)
d_o: Outer diameter of tube (mm)
e: Energy (kJ)
g: Acceleration due to gravity (m/s^2)
G_k: Production term for k (m^2/s^2)
G_b: Buoyancy term for TKE (m^2/s^2)
G_ε: Production term for ε (m^2/s^3)
h: Convective heat transfer coefficient (W/m^2)
i, j: Loop indices
k: Turbulent kinetic energy (m^2/s^2)
L: Length of heat exchanger (mm)
N_b: Number of baffles
N_t: Number of tubes
T: Temperature (°C)
T_{cin}: Temperature of cold fluid (°C)
T_{hin}: Temperature of hot fluid (°C)
P: Pressure (Pa)
q: Heat flux (kW/m^2)
u, v, w: Velocity components (m/s)
CFD: Computational fluid dynamics

STHX: Shell-and-tube heat exchanger
atm: Atmosphere
: **Greek Symbols**
ϕ: Viscous dissipation function
τ_{xy}: Viscous shear stress (Pa)
λ: Second coeff. of viscosity (kg/m-s)
μ_t: Turbulent viscosity (kg/m-s)
μ: Dynamic viscosity (kg/m-s)
ε: Dissipation rate (m^2/s^3)
ρ: Density (kg/m^3)
σ_k: Turbulent Prandtl number for k
σ_ε: Turbulent Prandtl number for ε
∇: Del operator.

Data Availability

The data used to support the findings of this study are available from the corresponding author upon request.

Conflicts of Interest

The authors declare that they have no conflicts of interest.

Acknowledgments

The authors wish to acknowledge the Department of RIC, IKGPTU, Punjab, India, for providing opportunity to conduct this research.

References

[1] B. Sundén, "Computational fluid dynamics in research and design of heat exchangers," *Heat Transfer Engineering*, vol. 28, no. 11, pp. 898–910, 2007.

[2] S. A. Payambarpour, H. Shokouhmand, M. H. Ahmadi, M. El Haj Assad, and L. Chen, "Effect of wetness pattern on the fin-tube heat exchanger performance under partially wet-surface condition," *Thermal Science and Engineering Progress*, vol. 19, Article ID 100619, 2020.

[3] W. H. Alawee, H. A. Dhahad, and K. I. Abass, "Increase the yield of simple solar distillation using the water drip method," *International Journal of Computation and Applied Sciences*, vol. 6, no. 2, pp. 447–445, 2019.

[4] K. J. Bell, "Heat exchanger design for the process industries," *Journal of Heat Transfer*, vol. 126, no. 6, pp. 877–885, 2005.

[5] L. Bellahcene, D. Sahel, and A. Yousfi, "Numerical study of shell and tube heat exchanger performance enhancement using nanofluids and baffling technique," *Journal of Advanced Research in Fluid Mechanics and Thermal Sciences*, vol. 80, no. 2, pp. 42–55, 2021.

[6] S. A. Payambarpour, M. Alhuyi Nazari, M. H. Ahmadi, and A. J. Chamkha, "Effect of partially wet-surface condition on the performance of fin-tube heat exchanger," *International Journal of Numerical Methods for Heat & Fluid Flow*, vol. 29, 2019.

[7] B. B. Gulyani, "Estimating number of shells in shell and tube heat exchangers: a new approach based on temperature cross," *Journal of Heat Transfer*, vol. 122, no. 3, pp. 566–571, 2000.

[8] E. Ozden and I. Tari, "Shell side CFD analysis of a small shell-and-tube heat exchanger," *Energy Conversion and Management*, vol. 51, no. 5, pp. 1004–1014, 2010.

[9] A. M. Ez Abadi, M. Sadi, M. Farzaneh-Gord, M. H. Ahmadi, R. Kumar, and K.-w. Chau, "A numerical and experimental study on the energy efficiency of a regenerative Heat and Mass Exchanger utilizing the counter-flow Maisotsenko cycle," *Engineering Applications of Computational Fluid Mechanics*, vol. 14, no. 1, pp. 1–12, 2020.

[10] M. Kahani, M. H. Ahmadi, A. Tatar, and M. Sadeghzadeh, "Development of multilayer perceptron artificial neural network (MLP-ANN) and least square support vector machine (LSSVM) models to predict Nusselt number and pressure drop of TiO $_2$/water nanofluid flows through non-straight pathways," *Numerical Heat Transfer, Part A: Applications*, vol. 74, pp. 1–17, 2018.

[11] H. Maddah, R. Aghayari, M. Mirzaee, M. H. Ahmadi, M. Sadeghzadeh, and A. J. Chamkha, "Factorial experimental design for the thermal performance of a double pipe heat exchanger using Al2O3-TiO2 hybrid nanofluid," *International Communications in Heat and Mass Transfer*, vol. 97, pp. 92–102, 2018.

[12] E. Jamalei, R. Alayi, A. Kasaeian, F. Kasaeian, and M. H. Ahmadi, "Numerical and experimental study of a jet impinging with axial symmetry with a set of heat exchanger tubes," *Mech India*, vol. 19, 2018.

[13] A. A. Bhuiyan and A. K. M. S. Islam, "Thermal and hydraulic performance of finned-tube heat exchangers under different flow ranges: a review on modeling and experiment," *International Journal of Heat and Mass Transfer*, vol. 101, pp. 38–59, 2016.

[14] A. L. H. Costa and E. M. Queiroz, "Design optimization of shell-and-tube heat exchangers," *Applied Thermal Engineering*, vol. 28, no. 14-15, pp. 1798–1805, 2008.

[15] A. Falav Jozaei, A. Baheri, M. K. Hafshejani, and A. Arad, "Optimization of baffle spacingon heat transfer, pressure drop and estimated price in a shell-and-tube heat exchanger," *World Applied Sciences Journal*, vol. 18, pp. 1727–1736, 2012.

[16] H. Li and V. Kottke, "Effect of baffle spacing on pressure drop and local heat transfer in shell-and-tube heat exchangers for staggered tube arrangement," *International Journal of Heatx and Mass Transfer*, vol. 41, no. 10, pp. 1303–1311, 1998.

[17] D. Rai, S. Bharati, and S. Bux, "To study of parametric analysis of shell and tube heat exchanger," *International Journal of Advance Research and Innovative Ideas*, vol. 1, pp. 383–391, 2015.

[18] D. S. Patel, R. R. Parmar, and V. M. Prajapati, "CFD analysis of shell and tube heat exchangers–a review," *International Research Journal of Engineering and Technology*, vol. 17, 2015.

[19] B. T. Lebele-Alawa and V. Egwanwo, "Numerical Analysis of the Heat Transfer in Heat Exchangers," *Journal of Engineering Physics and Thermophysics*, vol. 2, pp. 1–5, 2009.

[20] V. K. Chalwa and N. Kadli, "Study of variation for pressure drop and temperature distribution in a shell and tube heat exchanger in case of vertical baffle," *Mechanica Confab*, vol. 2, pp. 17–25, 2013.

[21] K. Anand, V. K. Pravin, and P. H. Veena, "Experimental investigation of shell and tube heat exchanger using Bell Delaware," *Method*, vol. 2, pp. 73–85, 2014.

[22] J. Yang, L. Ma, J. Bock, A. M. Jacobi, and W. Liu, "A comparison of four numerical modeling approaches for enhanced shell-and-tube heat exchangers with experimental validation," *Applied Thermal Engineering*, vol. 65, no. 1-2, pp. 369–383, 2014.

[23] S. Wang, J. Wen, and Y. Li, "An experimental investigation of heat transfer enhancement for a shell-and-tube heat

exchanger," *Applied Thermal Engineering*, vol. 29, no. 11-12, pp. 2433–2438, 2009.

[24] A. Ramezanpour, I. Mirzaee, R. Rahmani, and H. Shirvani, "Numerical study of staggered tube bundle in turbulent cross flow for an optimum arrangement," *International Journal of Heat and Mass Transfer*, vol. 7, pp. 37–56, 2006.

[25] K. M. Kwak, K. Torii, and K. Nishino, "Heat transfer and pressure loss penalty for the number of tube rows of staggered finned-tube bundles with a single transverse row of winglets," *International Journal of Heat and Mass Transfer*, vol. 46, no. 1, pp. 175–180, 2003.

[26] S. B. Beale and D. B. Spalding, "A Numerical study of unsteady fluid flow in in-line and staggered tube banks," *Journal of Fluids and Structures*, vol. 13, no. 6, pp. 723–754, 1999.

[27] T. Shaligram, "Numerical study of heat transfer and pressure drop for flow past inline and staggered tube bundles," *International Journal of Numerical Methods for Heat & luid Flow*, vol. 19, pp. 931–949, 2009.

[28] J. M. Hassan, T. A. Mohamed, W. S. Mohammed, and W. H. Alawee, "Experimental and numerical study on the improvement of uniformity flow for three-lateral dividing manifold," in *Proceedings of the World Research and Innovation Convention on Engineering and Technology*, Putrajaya, Malaysia, February 2014.

[29] W. H. Alawee, J. M. Hassan, and W. S. Mohammad, "Experimental and numerical study on the improvement of uniformity flow in a parallel flow channel," *Eng. Technol. J.*vol. 34, pp. 847–856, 2016.

[30] W. H. Alawee, G. F. Al-Sumaily, H. A. Dhahad, and M. C. Thompson, "Numerical analysis of non-Darcian mixed convection flows in a ventilated enclosure filled with a fluid-saturated porous medium," *Thermal Science and Engineering Progress*, vol. 24, Article ID 100922, 2021.

[31] G. F. Al-Sumaily, H. M. Hussen, W. H. Alawee, H. A. Dhahad, and M. C. Thompson, "Non-Darcian Bénard convection in eccentric annuli containing spherical particles," *International Journal of Heat and Fluid Flow*, vol. 86, Article ID 108705, 2020.

[32] W. H. Alawee, B. Yusuf, T. A. Mohammad, and H. A. Dhahad, "Variation of flow along a multiple outlets pipe with various spacing and inflow water head based on physical model," *Journal of Engineering Science and Technology*, vol. 14, pp. 2399–2409, 2019.

[33] J. M. Hassan, W. S. Mohammed, T. A. Mohamed, and W. H. Alawee, "CFD simulation for manifold with tapered longitudinal section," *International Journal of Emerging Technology and Advanced Engineering*, vol. 4, pp. 28–35, 2014.

[34] P. Singh, N. K. Grover, V. Agarwal et al., "Computational fluid dynamics analysis of impingement heat transfer in an inline array of multiple jets," *Mathematical Problems in Engineering*, vol. 2021, Article ID 6668942, 10 pages, 2021.